Available online at www.sciencedirect.com

ScienceDirect

Procedia Engineering 159 (2016) 94 – 103

Procedia Engineering

www.elsevier.com/locate/procedia

Humanitarian Technology: Science, Systems and Global Impact 2016, HumTech2016

Towards a Real-time Measurement Platform for Microgrids in Isolated Communities.

Geir Kulia[a,*], Marta Molinas[b], Lars Lundheim[a], Bjørn B. Larsen[a]

[a] *Department of Electronics and Telecommunications, NTNU, 7491 Trondheim*
[b] *Department of Engineering Cybernetics, NTNU, 7491 Trondheim*

Abstract

This paper describes a platform for obtaining and analyzing real-time measurements in Microgrids. A key building block in this platform is the Empirical Mode Decomposition (EMD) used to analyze the electrical voltage and current waveforms to identify the instantaneous frequency and amplitude of the monocomponents of the original signal. The method was used to analyse the frequency fluctuation and obtain information about the linearity of electrical current and voltage waveforms measured in the field. Comparison between grid-connected and stand-alone microgrid voltage and currents' monocomponents were conducted. Fluctuations in the grid frequency occurred in both the grid-connected and stand-alone microgrid, but the degree of the observed fluctuations were different, revealing more apparent nonlinear distortions in the latter. The observed instantaneous frequency from the collected data indicates potential nonstationary electrical signals when compared to synthetic data containing periodic signals coming from nonlinear loads. This observation leads us to expect the next generation of real-time measuring devices for the micro power grids to be designed on the principle of instantaneous frequency detection. Further efforts will be directed to a more rigorous characterization of the nonstationary nature of the signals by analyzing more and longer set of data.

Peer-review under responsibility of the Organizing Committee of HumTech2016
Keywords: Instantaneous frequency, Hilbert-Huang Transform, Empirical mode decomposition, Microgrid, Frequency stability, Power systems

1. Introduction

Access to modern energy services is a necessity for economic development and particularly challenging in isolated communities. The fall in prices of photovoltaic (PV) cells opens the possibility for affordable, clean and sustainable energy to rural areas where, in most cases, extending the power grid is too expensive to be a realistic alternative. The nature of the location for such systems require near to maintenance free supervisory control systems. Good access to reliable data is essential to the supervisory control system to make correct actions. The nonlinearities of modern power electronic equipment and the stochastic nature of the photovoltaic sources of energy advocate the need for

* Corresponding author. Tel.: +47 992 99 867
E-mail address: geir@kulia.no

Peer-review under responsibility of the Organizing Committee of HumTech2016
doi:10.1016/j.proeng.2016.08.070

data acquisition systems based on real-time measurements and estimation of essential values, such as instantaneous amplitude and frequency. Existing measurement devices for microgrids do not fulfill this requirement, as they are generally based on average value calculations [1].

This paper explores methods for decomposing the electrical waveforms to extract their instantaneous frequency components. The frequency components are used to investigate the frequency stability of the waveforms. The resulting analysis will lay the foundation for future development of a real-time software platform for detection, analysis and correction capabilities for electrical waveform distortions in microgrid power systems, based on the principle of instantaneous frequency.

As physical data is the first step for a meaningful analysis, this project has, through a collaboration between Norwegian University of Science and Technology (NTNU) and the Royal University of Bhutan (RUB)'s College of Science and Technology, collected current and voltage measurements from two nearly identical systems: one was a grid-connected PV microgrid, and the other was the same PV microgrid in stand-alone mode. Voltage and current waveforms measured at Hundhammerfjellet windmill park in Norway were used as a reference for a qualitative comparison. The data obtained were analysed using the Hilbert-Huang Transform (HHT).

2. Analysis Method

The concept of instantaneous frequency and amplitude for a general signal is not well-defined. For near-sinusoidal signal shapes, such as those coming from a stable rotary generator, the instantaneous frequency can be associated with the rotational speed, and other variations could be ascribed to an instantaneous amplitude. In other situations with more complicated waveform, it is less clear how such parameters should be defined.

The voltage and current shapes studied in our context could be characterized as near periodic. In that case, using several (more or less) near-sinusoidal components, each with its own instantaneous frequency and amplitude is a possible approach. One method along these lines is the one suggested by Huang [2]. This approach, called the Hilbert-Huang Transform (HHT)[1], has been chosen for application on microgrid power systems in this paper, and is outlined in the following.

2.1. Instantaneous frequency

Any real signal $X(t)$ can be represented as an analytic signal $Z(t)$ in the form given by (1)

$$Z(t) = X(t) + jY(t) = a(t) \cdot e^{j\theta(t)} \tag{1}$$

where $Y(t)$ is the Hilbert transform of $X(t)$, $a(t)$ is the amplitude and $\theta(t)$ are the phase of $Z(t)$. From this, it is possible to define the instantaneous frequency of $X(t)$ as in (2) [2, pp. 911-915].

$$\omega(t) = \frac{d\theta(t)}{dt} \tag{2}$$

2.2. Hilbert-Huang Transform

Central to the HHT is the notion of Intrinsic Mode Functions (IMFs). An IMF is a function whose extrema are alternatingly positive and negative, i.e. there is always a zero crossing between each extremum. For such functions the instantaneous frequency will always be positive. By using a method called the Empirical Mode Decomposition (EMD) as described in [2, pp. 917-923] it is possible to decompose a genaral signal $s(t)$ into a set of IMFs, $c_1(t)$, $c_2(t)$,...,$c_N(t)$ such that

$$s(t) = r(t) + \sum_{i=1}^{N} c_i(t) \tag{3}$$

[1] The version of the method used in this paper was the Normalized Hilbert-Huang Transform [3, p. 15].

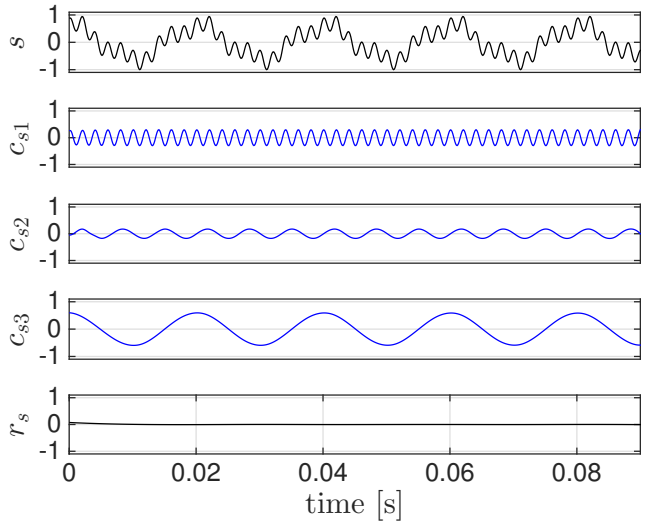

Fig. 1: Intrinsic mode functions and residue of $s(t)$ normalized between -1 and 1.

where $r(t)$ is a residual part of the signal that cannot be modeled as an IMF.

As an example of the EMD we will consider a normalized test signal $s(t)$. It's defined by (4) and corresponds to a three-term Fourier series.

$$s(t) = \cos(2\pi 50 \cdot t) + \frac{1}{3} \cdot \sin(2\pi 150 \cdot t) + \frac{1}{5} \cdot \cos(2\pi 500 \cdot t) \tag{4}$$

By applying the EMD on the simulated waveform $s(t)$ the IMFs were obtained. The IMFs of the signal $s(t)$ is depicted in fig. 1. The first row is the original signal. The intrinsic mode functions follow this. The first IMF, $c_1(t)$, has the highest frequency, the second, $c_2(t)$, has the second highest frequency and so on until the lowest frequency component. In this example, there are only three frequency components, i.e. $c_{s1}(t)$, $c_{s2}(t)$, and $c_{s3}(t)$. The sum of all the IMFs should ideally be equal to the raw data. For electrical systems, the last IMF ($c_{s3}(t)$ for $s(t)$) is the grid frequency, i.e. the 50 Hz sine component of the signal. The previous IMFs contain all distortions, such as noise and harmonics.

2.3. Hilbert Spectrum

The Hilbert Spectrum is a way to represent the instantaneous frequency and amplitude as a function of time for all IMFs. By applying the EMD the intrinsic mode function of the signal are obtained. Each IMF, $c_i(t)$, can be represented as an analytic signal, $Z_i(t)$ as shown in (1), with the amplitude $a_i(t)$, and frequency $\omega_i(t)$ as defined in (2). Equation (5) shows the definition of the Hilbert spectrum, $H_i(\omega, t)$, for a given IMF, c_i.

$$H_i(\omega, t) = \begin{cases} a_i(t) & \text{for } \omega = \omega_i(t) \\ 0 & \text{otherwise} \end{cases} \tag{5}$$

Fig. 2(a) displays the Hilbert spectrum of $s(t)$'s third intrinsic mode function, $c_3(t)$. It is possible to obtain the Hilbert spectrum of any signal by summing all the intrinsic mode functions as shown in (6).

$$H(\omega, t) = \sum_{i=1}^{N} H_i(\omega, t) \tag{6}$$

The Hilbert spectrum, H_s, of $s(t)$, is depicted in fig. 2(b). For all Hilbert spectra in this paper, the amplitudes are normalized between -1 and 1, such that 0 dB = 1.

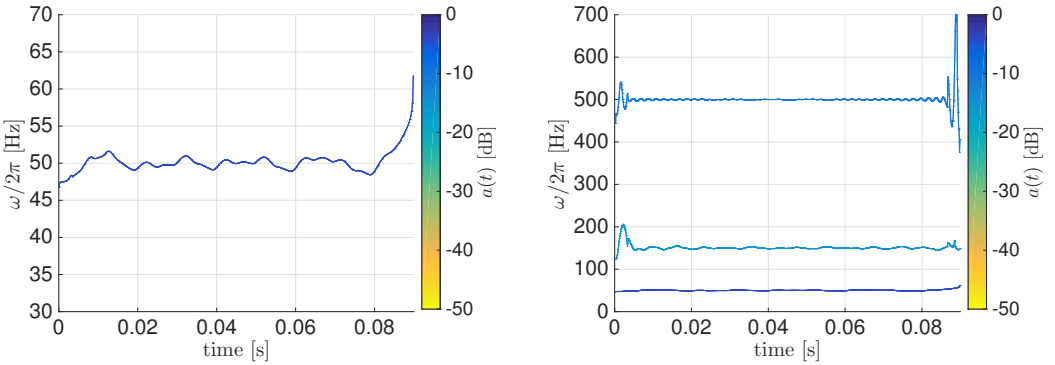

(a) Hilbert spectrum of $s(t)$'s third intrinsic mode function, $c_{s3}(t)$.

(b) Hilbert spectrum of $s(t)$.

Fig. 2: Hilbert spectra of s(t)

Table 1: Summary of frequency fluctuations on the generated test signal $s(t)$.

	c_{s3}	c_{s2}	c_{s1}
Mean frequency	49.96 Hz	150.10 Hz	499.99 Hz
Max frequency	51.12 Hz	153.16 Hz	501.35 Hz
Min frequency	49.12 Hz	147.79 Hz	498.49 Hz
Deviation from mean frequency	2.32 %	2.04 %	0.30 %

The generated test signal $s(t)$ should be represented as perfect, horisontal lines in the frequency spectrum. Fig. 2 shows ripples on s(t) up to 2.32 % (see table 1). This is an error introduced by the implementation of the method. 20 ms of samples on the start and end of the signals were discarded from the summary in the tables to remedy for end-effects when calculating the instantanious frequency.

3. Measurements

Electrical current and voltage measurements were performed at RUB College of Science and Technology's two PV microgrids. The grids are similar, with the exception that one is connected to the public power grid while the other is not. Fig. 4(a) and 4(b) shows the grid-connected and stand-alone microgrid respectively. The load is the load impedance of the parts of the college that the microgrid provide with electricity.

The point of measurements is marked on both figures. The resulting measurements of the electrical voltage and current waveforms are displayed in fig. 3.

Measurements of the Norwegian grid, shown in fig. 3(a) and 3(b), was used as a reference. The measurements were conducted by Sintef Energi AS at Hundhammerfjellet windmill park.

The voltage waveforms should ideally be pure 50 Hz sine waves. Harmonics on the power system is caused by nonlinear loads and is undesirable. By visual inspection, it is apparent that the waveforms measured in Bhutan are far more distorted compared to the waveforms measured in Norway. It is also evident that the stand-alone microgrid has more distortions compared to the grid-connected one.

All the measurements are normalized between -1 and 1.

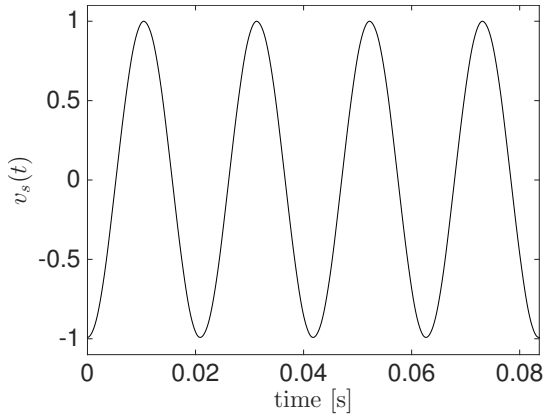

(a) Normalized voltage measured, v_s, at Hundhammerfjellet windmill park, Norway.

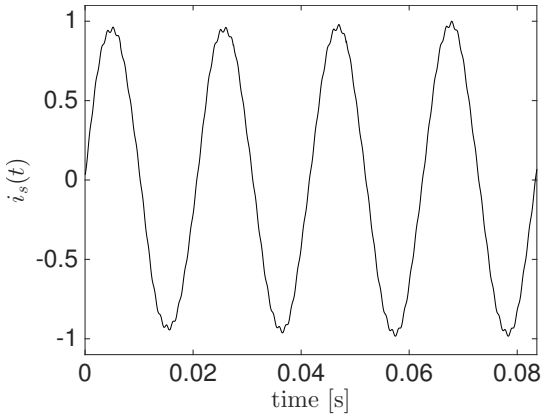

(b) Normalized current measured, i_s, at Hundhammerfjellet windmill park, Norway.

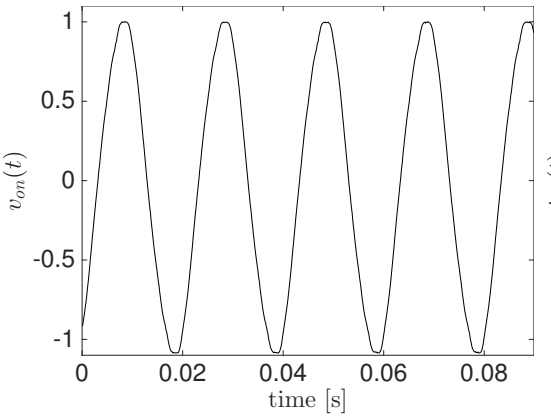

(c) Normalized voltage, v_{on}, measured at the grid-connected microgrid (see setup in fig. 4(a)).

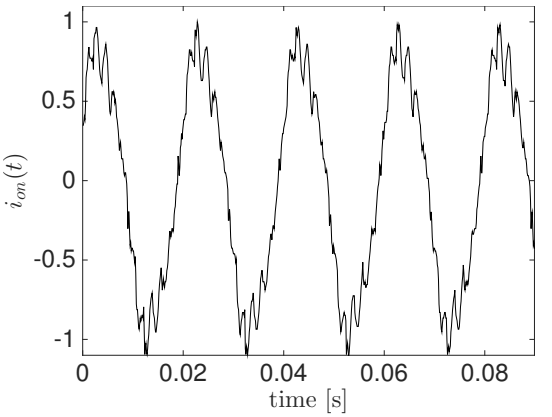

(d) Normalized current, i_{on}, measured at the grid-connected microgrid (see setup in fig. 4(a)).

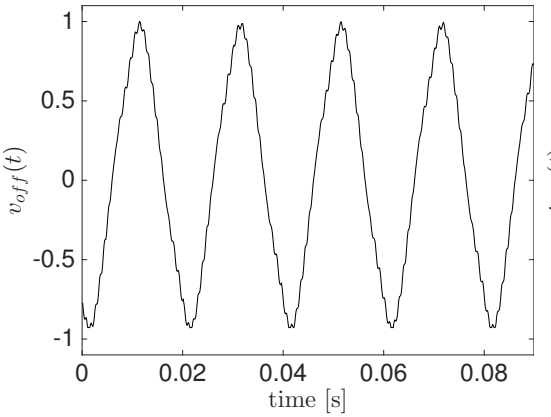

(e) Normalized voltage, v_{off}, measured at the standalone microgrid (see setup in fig. 4(b)).

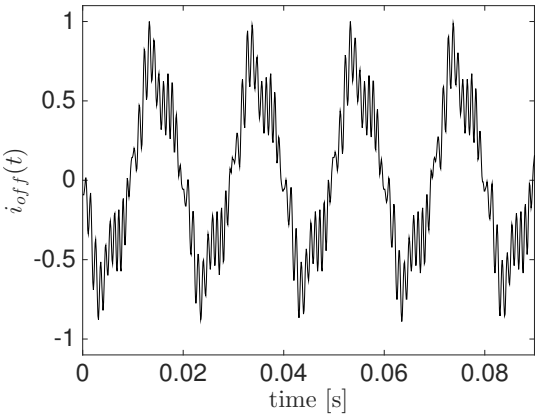

(f) Normalized current, i_{off}, measured at the standalone microgrid (see setup in fig. 4(b)).

Fig. 3: Electrical waveforms measured.

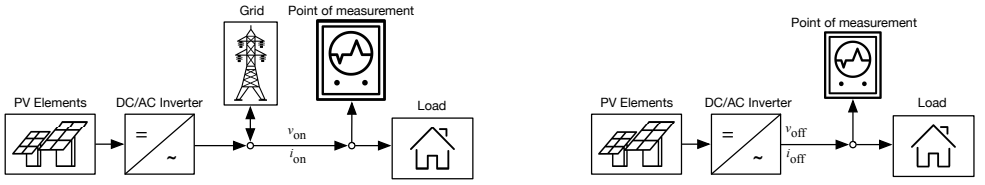

(a) Voltage and current measurement setup for a grid-connected PV-microgrid.

(b) Voltage and current measurement setup for a stand alone PV-microgrid.

Fig. 4: The two different voltage and current measurement setups.

Table 2: Summary of frequency fluctuations measured at Hundhammerfjellet windmill park.

	$c_{v_s}1$	$c_{i_s}2$
Mean frequency	47.75 Hz	47.80 Hz
Max frequency	48.89 Hz	51.72 Hz
Min frequency	46.53 Hz	44.76 Hz
Deviation from mean frequency	2.57 %	8.2074 %

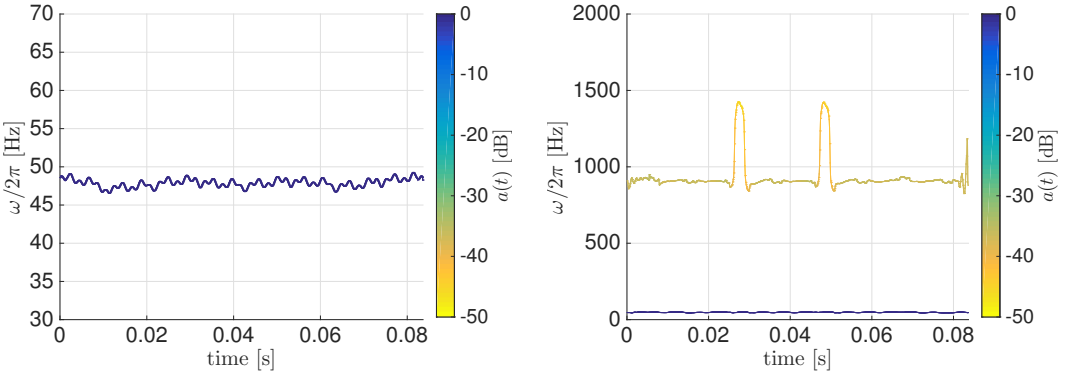

(a) Hilbert spectrum of $v_s(t)$.

(b) Hilbert spectrum of $i_s(t)$.

Fig. 5: Hilbert spectra of electrical waveform data collected at Hundhammerfjellet windmill park, $v_s(t)$ and $i_s(t)$.

4. Results

4.1. Analysis of electrical waveform data collected at Hundhammerfjellet windmill park, Norway

The voltage and current waveforms collected at Hundhammerfjellet windmill park in Norway, $v_s(t)$ and $i_s(t)$, were analyzed using the Hilbert-Huang transform. Their Hilbert spectra are shown in fig. 5. $v_s(t)$ is a monocomponent signal and have therefore only one IMF, $c_{v_s}1(t) = v_s(t)$. The fluctuation of the instantaneous frequency was measured and a summary is shown in table 2. The frequency fluctuations observed on $v_s(t)$ are relatively modest, and slightly higher than the frequency fluctuation artifacts introduced on $s(t)$. It's important to note that the mean frequency measured using HHT is 47.75 Hz, while it was 50 Hz using zero crossing frequency. While our current implementation of HHT can analyze frequency patterns, it often struggles to determin the exact frequency values for short samples.

In contrast, $i_s(t)$ consists of two IMF, $c_{i_s}1(t)$ and $c_{i_s}2(t)$. The first intrinsic mode function, $c_{i_s}1(t)$, contains all harmonics and other distortions of $i_s(t)$. It's showed by the yellow graph on the Hilbert Spectrum in fig. 5(b). $c_{i_s}1(t)$'s amplitude is low and always below -35 dB. It has two spikes with increased frequency, that most probably is caused by nonlinear loads, i.e. loads that draw a nonsinusoidal current from a sinusoidal voltage source [4].

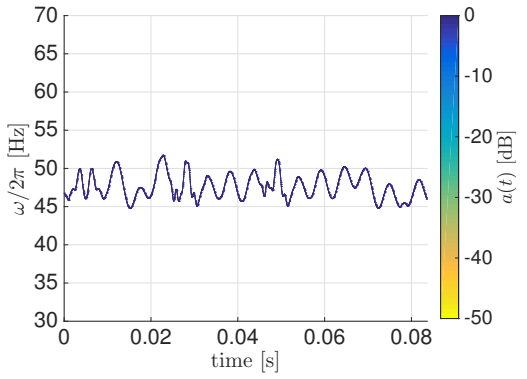

Fig. 6: Hilbert spectrum of $c_{i_s2}(t)$.

Table 3: Summary of frequency fluctuations measured at the grid-connected microgrid.

	$c_{v_{\text{on}}6}$	$c_{i_{\text{on}}6}$
Mean frequency	49.65 Hz	49.26 Hz
Max frequency	54.31 Hz	64.63 Hz
Min frequency	45.65 Hz	37.86 Hz
Deviation from mean frequency	9.38 %	31.18 %

$i_s(t)$'s second intrinsic mode function, $c_{i_s2}(t)$ is the blue graph located around 50 Hz. Table 2 shows that it has considerable more variations in it's frequency than $c_{v_s1}(t)$. It is expected that the current is more distorted compared to its corresponding voltage source. Both the frequency fluctuations on $c_{i_s2}(t)$ and $c_{v_s1}(t)$ have a high periodic behavior.

4.2. Analysis of electrical waveform data collected at the grid-connected microgrid

The voltage waveform, $v_{\text{on}}(t)$, measured at the grid-connected microgrid was decomposed into six IMFs, $c_{v_{\text{on}}1}$ to $c_{v_{\text{on}}6}$, where $c_{v_{\text{on}}6}$ corresponds to the grid frequency. The three first IMFs, $c_{v_{\text{on}}1}$ to $c_{v_{\text{on}}3}$, were discarded as their frequency fluctuations are higher than the band limit described in [2, p. 929]. The summary of the fluctuations in the grid frequency is shown in table 3. The frequency variations on $v_{\text{on}}(t)$ are 3.65 times higher than that on $v_s(t)$, with fluctuations up to 9.37 % from the mean. From fig. 7(a) it is notable to see that the frequency has a periodic behavior, with a new cycle every 10 ms.

The Hilbert spectrum of $v_{\text{on}}(t)$ is shown in fig. 8(a) and shows considerable distortions. In this figure, the blue line at the bottom is $c_{v_{\text{on}}6}$, the graph shifting between blue-green and yellow is $c_{v_{\text{on}}5}$, and the yellow graph at the top is $c_{v_{\text{on}}3}$.

The corresponding current waveform, $i_{\text{on}}(t)$, was divided into seven IMFs, $c_{i_{\text{on}}1}$ to $c_{i_{\text{on}}7}$, where the first two IMFs were discarded due to reasons described above. $i_{\text{on}}(t)$'s Hilbert spectrum is depicted in fig. 8(b). The light blue, green and orange graphs above it corresponds to higher frequency distortions and is represented by the first six IMFs, $c_{i_{\text{on}}1}$ to $c_{i_{\text{on}}6}$. These have amplitudes up to -21 dB, so frequency fluctuations on $i_{\text{on}}(t)$ has a higher magnitude than $i_s(t)$'s.

The blue line at the bottom of the Hilbert spectrum corresponds to the 50 Hz of the current $i_{\text{on}}(t)$, i.e. $c_{i_{\text{on}}7}$. As observed, $c_{i_{\text{on}}7}$'s instantaneous frequency also has a periodic behavior, with frequency cycles of 10 ms, just like $c_{v_{\text{on}}6}$ (see fig. 7(b)). This is probably a cause for much of the distortions on $v_{\text{on}}(t)$.

The observed 100 Hz instantaneous frequency is a property of the instantaneous power in single phase alternating current systems. This effect being observed in the voltage and current might indicate a propagation of the power oscillations on the ac side through the inverter dc bus voltage and the control feedback of the inverter. To elucidate the nature of this instantaneous frequency transfer from the power to the voltage and current, further efforts will be directed towards matching this measured 100 Hz instantaneous frequency with an analytical model of the votlage and current of the inverter.

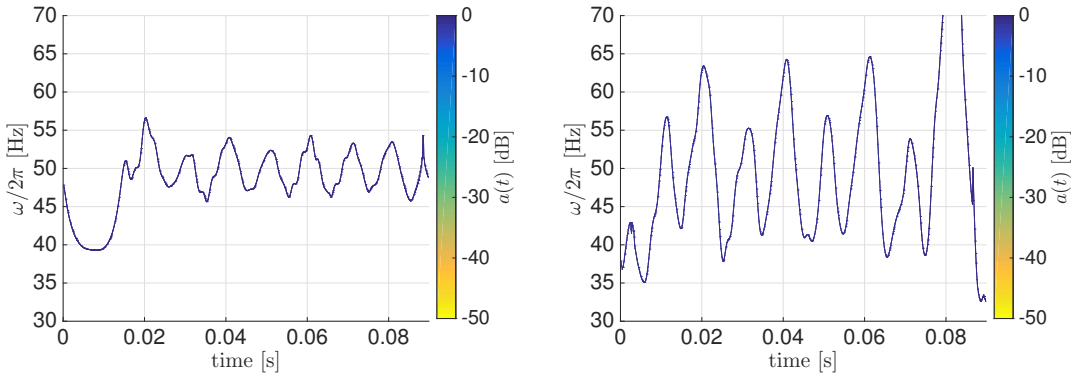

(a) Hilbert spectrum of $c_{v_{\text{on}}6}(t)$. **(b)** Hilbert spectrum of $c_{i_{\text{on}}6}(t)$.

Fig. 7: Grid frequency of $v_{\text{on}}(t)$ and $i_{\text{on}}(t)$.

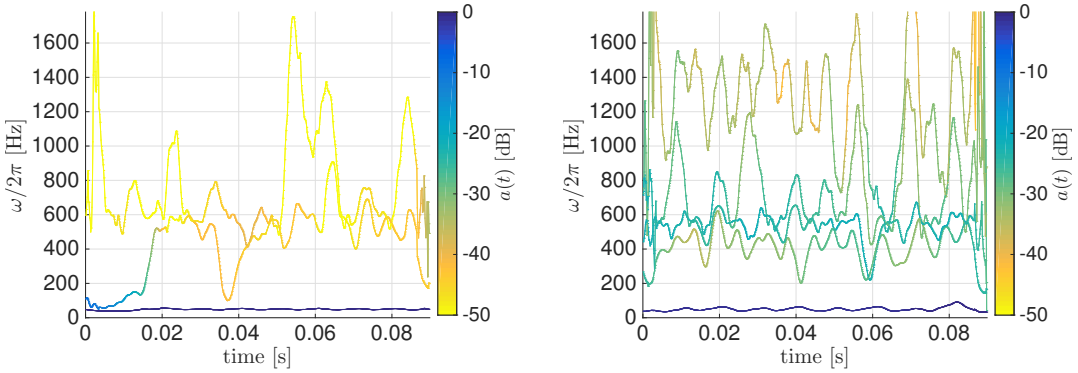

(a) Hilbert spectrum of $v_{\text{on}}(t)$. **(b)** Hilbert spectrum of $i_{\text{on}}(t)$.

Fig. 8: Hilbert spectra of electrical waveforms measured at grid-connected microgrid.

Table 4: Summary of frequency fluctuations measured at the stand alone micromicrogrid.

	$c_{v_{\text{off}}3}$	$c_{i_{\text{off}}6}$
Mean frequency	50.04 Hz	49.48 Hz
Max frequency	58.10 Hz	64.09 Hz
Min frequency	41.25 Hz	33.98 Hz
Deviation from mean frequency	17.56 %	31.33 %

4.3. Analysis of electrical waveform data collected at the stand-alone microgrid

The voltage waveform $v_{\text{off}}(t)$ measured at the stand alone microgrid was decomposed like $v_{\text{on}}(t)$, into IMFs. Three IMFs, $c_{v_{\text{off}}1}$ to $c_{v_{\text{off}}3}$, were necessary to describe $v_{\text{off}}(t)$. Unlike $v_{\text{on}}(t)$, none of $v_{\text{off}}(t)$'s IMFs were discarded. The Hilbert spectrum of $v_{\text{off}}(t)$ is shown in fig. 10(a). The blue line at the bottom represent the grid frequency, $c_{v_{\text{off}}3}$. The yellow graph above it represent $c_{v_{\text{off}}2}$ and the brown graph at the top is $c_{v_{\text{off}}1}$. $c_{v_{\text{off}}1}$'s frequency has periodic properties with cycles of 10 ms, and an amplitude up to -34 dB. As shown in fig. 9(a), $c_{v_{\text{off}}3}$ does also have frequency fluctuations with periods of 10 ms, but its frequency cycles are phase shifted, compared to that of $c_{v_{\text{off}}1}$'s instantanious frequency. The magnitude of the frequency fluctuations on $c_{v_{\text{off}}3}$ is 1.87 and 6.83 times higher than that observed on $c_{v_{\text{on}}6}$ and c_{v_s1} respectively.

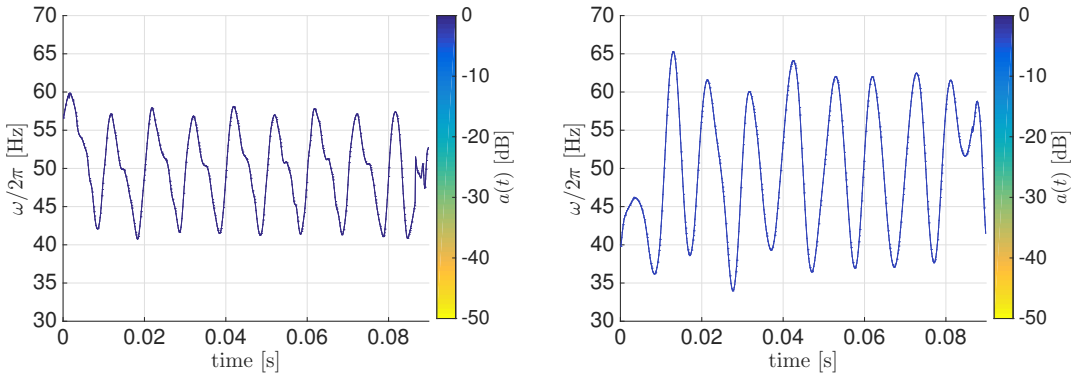

(a) Hilbert spectrum of $c_{v_{\text{off}}3}(t)$.

(b) Hilbert spectrum of $c_{i_{\text{off}}6}(t)$.

Fig. 9: Grid frequency of $v_{\text{off}}(t)$ and $i_{\text{off}}(t)$.

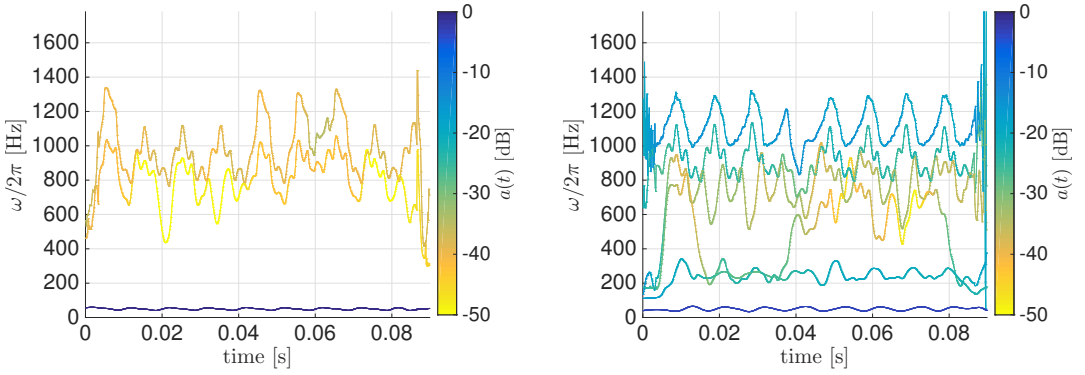

(a) Hilbert spectrum of $v_{\text{off}}(t)$.

(b) Hilbert spectrum of $i_{\text{off}}(t)$.

Fig. 10: Hilbert spectra of electrical waveforms measured at the stand-alone microgrid.

The corresponding current waveform, $i_{\text{off}}(t)$, was decomposed to six IMFs, $c_{i_{\text{on}}1}$ to $c_{i_{\text{on}}6}$. The Hilbert spectrum of $i_{\text{off}}(t)$ is shown in fig. 10(b). The first IMF $c_{i_{\text{on}}1}$ is the light blue graph at the top of the Hilbert spectrum. Its amplitude peaks at -15 dB, and the frequency has varying cycles with a period around 10 ms, that are phase shifted to $c_{v_{\text{off}}3}$'s frequency cycles. $c_{i_{\text{off}}2}$ has similar frequency cycles. The last IMF, $c_{i_{\text{off}}6}$, corresponds to the 50 Hz component of the signal. Its frequency also varies with cycles of 10 ms (see fig. 9(b)).

It is remarkable how much more distorted the stand-alone grid is compared to the grid-connected one. It is also noteworthy that also in this case there is a systematic 10 ms fluctuation on the stand alone microgrid as the one observed in the grid connected microgrid. As explained above, this originates from the typical 100 Hz oscillations observed in the power of single phase systems [4].

5. Discussion

Foundations for a software platform for real-time data acquisition and analysis of distorted electrical measurements for isolated microgrids have been outlined in this paper. The HHT-EMD lies at the core of this platform by enabling the identification of instantaneous frequencies in the monocomponents of the original data. The Empirical Mode Decomposition divides the electrical voltage and current waveforms into useful and easy-to-analyze modes, where each component carries information about particular aspects of the signal and the system behind the signal. Showing that the instantaneous grid frequency is not stable with considerable fluctuations on both grids connected and stand

alone microgrids displays the strength of the method, which has enabled us to identify a transfer of frequency (10 ms Cycle) from the power to the voltage and currents of the microgrid. A similar identification was not possible to achieve with an FFT analysis of the data. An apparent difference that emerges from our comparison is the characteristics of the frequency fluctuation of the synthetically generated data and the field data. The synthetic data shows periodic characteristics with constant frequency while the field data appears to have high-frequency fluctuations. Further efforts will be put in distinguishing this difference more categorically by analyzing data more extensively.

From these results, we expect that measurement equipment able to acquire, analyze and detect electrical grid problems in the types of grid studied in this paper, will require information about the instantaneous values of frequencies of the monocomponents of the signal. Our results also indicate that tools such as the EMD will provide a better understanding of the electrical waveforms, enabling in the future, better and more accessible microgrid control possibilities.

Acknowledgments

This research was partially supported by Ren-Peace, IUG NTNU, and Department of Electronics and Telecommunications at NTNU.

We thank Norden Huang who provided insight and expertise in his methods by spending tens of hours teaching and discussing them with us. His open-mindedness and generosity have been a tremendous source of inspiration.

The data analysis would not have been verified without the measurements preformed at RUB. It is therefore in place to thank Tshewang Lhendupand, Cheku Dorji and my travel partner and coworker Håkon Duus for their assistance in collecting data from the microgrids.

We would also like to acknowledge the contribution of Helge Seljeseth at Sintef AS for providing data from Hundhammerfjellet windmill park.

The icons in fig. 4 were designed by Freepik.

References

[1] IEEE Standard 519, *IEEE Recommended Practice and Requirements for Harmonic Control in Electric Power Systems*, New York, IEEE Power Energy Society, 2014

[2] Norden E. Huang, Zheng Shen, Steven R. Long, Manli C. Wu, Hsing H. Shih, Quanan Zheng, Nai-Chyuan Yen, Chi Chao Tung and Henry H. Liu, *The Empirical Mode Decomposition and the Hilbert Spectrum for Nonlinear and Non-Stationary Time Series Analysis*, London, United Kingdom, Royal Society, 1996

[3] Norden E. Huang, Samuel S. P. Shen *Hilbert-Huang Transform and Its Applications*, 2nd ed. Singapore, World Scientific publisher Co. Pte. Ltd., 2014

[4] Hirofumi Akagi, Edson Hirokazu Watanabe, Mauricio Aredes, *Instantaneous Power Theory and Applications to Power Conditioning*, IEEE Computer Society Press, New York, Wiley, 2007

[5] Mohan, Undeland, Robbins, *Power electronics - Converters, Applications, and Design*, 3rd ed. New York, Wiley, 2003